# A Dynamic Physicochemical Model for Chemical Phosphorus Removal

7 authors, including:

**Hélène Hauduc**
Dynamita SARL, France
**18** PUBLICATIONS **250** CITATIONS

SEE PROFILE

**Scott Smith**
Wilfrid Laurier University
**66** PUBLICATIONS **1,661** CITATIONS

SEE PROFILE

**Glen T Daigger**
University of Michigan
**260** PUBLICATIONS **3,744** CITATIONS

SEE PROFILE

**Mathieu Spérandio**
Institut National des Sciences Appliquées de …
**95** PUBLICATIONS **1,633** CITATIONS

SEE PROFILE

Some of the authors of this publication are also working on these related projects:
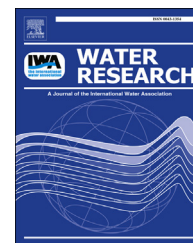
Project Good Modelling Practice View project

Project Biofilm Reactor Modeling View project

CrossMark

# A dynamic physicochemical model for chemical phosphorus removal

H. Hauduc [a,b,c,*], I. Takács [d], S. Smith [e], A. Szabo [f], S. Murthy [g], G.T. Daigger [h], M. Spérandio [a,b,c]

[a] Université de Toulouse, INSA, UPS, INP, LISBP 135 Avenue de Rangueil, F-31077 Toulouse, France
[b] INRA, UMR792 Ingénierie des Systèmes Biologiques et des Procédés, F-31400 Toulouse, France
[c] CNRS, UMR5504, F-31400 Toulouse, France
[d] Dynamita, Nyons, France
[e] Wilfrid Laurier University, Waterloo, Ontario, Canada
[f] Inno-Water Ltd., Budapest, Hungary
[g] DCWater, Washington, DC, USA
[h] CH2MHill, Denver, CO, USA

## ARTICLE INFO

## ABSTRACT

A dynamic physico-chemical model for chemical phosphorus removal in wastewater is presented as a tool to optimize chemical dosing simultaneously while ensuring compliant effluent phosphorus concentration. This new model predicts the kinetic and stoichiometric variable processes of precipitation of hydrous ferric oxides (HFO), phosphates adsorption and co-precipitation. It is combined with chemical equilibrium and physical precipitation reactions in order to model observed bulk dynamics in terms of pH. The model is calibrated and validated based on previous studies and experimental data from Smith et al. (2008) and Szabo et al. (2008) as a first step for full-plant implementation. The simulation results show that the structure of the model describes adequately the mechanisms of adsorption and co-precipitation of phosphate species onto HFO and that the model is robust under various experimental conditions.

© 2015 Elsevier Ltd. All rights reserved.

## 1. Introduction

Achieving phosphorus removal from wastewater to very low levels is often performed by metal salt addition. Iron dosage leads to rapid hydrous ferric oxide (HFO, close to 2-line ferrihydrite) precipitation. Phosphorus may then be removed from the bulk solution through different pathways: 1) adsorption of phosphates onto HFO by sharing an oxygen atom with iron; 2) co-precipitation of phosphate species into the HFO structure; 3) precipitation of ferric phosphate and 4) precipitation of mixed cation phosphates (Smith et al., 2008). The engineering stakes for this process consist of ensuring compliant effluent phosphorus concentrations, while at the same time saving

chemicals and limiting chemical sludge production. Furthermore, high doses of metal salts cause bulk pH decrease by metal hydrolysis reactions and decrease the buffer capacity due to phosphate entrapment (Caravelli et al., 2010) and carbon dioxide stripping.

Modelling is a commonly used engineering tool to handle such issues. However, metal salt precipitation such as iron dosing is not well described in current wastewater process models. Existing chemical phosphorus removal models are mainly focused on ferric phosphate precipitation (Fytianos et al., 1998). However, this pathway occurs only at acidic pH (below pH 5) as demonstrated by Smith et al. (2008) and based on literature solubility data (NIST, 2001). Luedecke et al. (1989) proposed an equilibrium model that includes acid/base reactions, hydrolysis of ferric ions and adsorption of phosphate on precipitates, considering an adsorption coefficient proportional to the ratio of the amount of adsorbed phosphates over the amount of adsorbent and the involved ions concentrations. However this ratio was adjusted to each experimental condition in a broad range ($0.28$–$4.3$ $e^{-12}$ $mol^2$ $L^{-2}$), indicating that the adsorption process is not correctly described. This can be partly explained by the variation of adsorption capacity of ferric compounds due to aging process demonstrated by Smith et al. (2008) and Bligh and Waite (2010). Therefore a new model is required to predict HFO precipitation, pH modifications through chemical equilibrium and phosphates adsorption and co-precipitation onto/into HFO.

The combination of very fast (chemical equilibrium) and slow (kinetic precipitation/adsorption) reactions, variable molar ratios, multiple dosage points, the effect of mixing, colloidal material conversions and multiple precipitates requires a new modelling framework. This framework can then be applied to full plant process models to optimize doses and dosage locations and increase the safety of effluent compliance. Consequently, a dynamic physicochemical model for chemical phosphorus removal was developed and calibrated based on previous studies and experimental data from Smith et al. (2008) and Szabo et al. (2008) as a first step before full-plant implementation. Furthermore, this study is focused on chemical phosphorus removal in aerobic plants and consequently on ferric iron ($Fe^{3+}$) processes.

## 2. Model development

A fully kinetic framework was used during development to simplify the model structure, meaning that chemical equilibrium dissociation processes are modelled dynamically with very fast rates as described in Musvoto et al. (2000). Five process types were included in the model: 1) chemical equilibrium dissociation (CED) processes (6 CED processes) that include water dissociation, carbonate, and phosphate acid-base systems. These kinetics are based on Loewenthal et al. (1989) and Musvoto et al. (2000); 2) chemical ion paring (CIP) processes (11 CIP processes) for ions present in the system (Fe, Ca) with kinetics based on Loewenthal et al. (1989) and Musvoto et al. (2000); 3) physical mineral precipitation (PMP) process (2 PMP process: HFO and FePO4 precipitation) with kinetic rate expressions built as in Musvoto et al. (2000); 4) chemical surface complexation (CSC) onto HFO processes (8 CSC processes) and 5) HFO aging processes (4 HFO processes).

All the reactions considered in the model are listed in Table 1, and the model concepts are described in more details below. The state variables related to these reactions are expressed in mol $L^{-1}$. The standardised notation from Corominas et al. (2010) has been used to name the state variables and parameters introduced in this model.

### 2.1. The physico-chemical model

The Gujer Matrix for the first two modules, namely the chemical equilibrium dissociation and chemical ion paring processes is presented in Appendix D. The kinetic rate expressions for chemical equilibrium dissociation are based on Musvoto et al. (2000), reverse and forward reactions being merged into a single process rate in order to reduce the number of modelled processes. The values of thermodynamic

**Table 1 − Reactions considered in the kinetic pH model, chemical ion paring and precipitation model.**

| **1) Chemical Equilibrium Dissociation** | | **3) Physical Mineral Precipitation** | |
|---|---|---|---|
| CED_01_H2O | $H_2O \leftrightarrow H^+ + OH^-$ | PMP_1_HFO_pre | $Fe(OH)_{3,aq} \leftrightarrow Fe(OH)_{3(s)}$ |
| CED_02_H2CO3 | $H_2CO_3 \leftrightarrow H^+ + HCO_3^-$ | PMP_2_FePO4 | $Fe^{3+} + PO_4^{3-} \leftrightarrow FePO_4$ |
| CED_03_HCO3 | $HCO_3^- \leftrightarrow H^+ + CO_3^{2-}$ | | |
| CED_04_H3PO4 | $H_3PO_4 \leftrightarrow H^+ + H_2PO_4^-$ | **4) Chemical Surface Complexation** | |
| CED_05_H2PO4 | $H_2PO_4^- \leftrightarrow H^+ + HPO_4^{2-}$ | CSC_01_HFOH_HPO4 | adsorption of |
| CED_06_HPO4 | $HPO_4^{2-} \leftrightarrow H^+ + PO_4^{3-}$ | CSC_02_HFOH_H2PO4 | phosphates onto |
| **2) Chemical Ion Paring** | | CSC_03_HFOH_H3PO4 | $X_{HFO,H}$ |
| CIP_01_CaOH | $Ca^{2+} + OH^- \leftrightarrow CaOH^+$ | CSC_04_HFOH_H | Protonation of $X_{HFO,H}$ |
| CIP_02_CaCO3 | $Ca^{2+} + CO_3^{2-} \leftrightarrow CaCO_3$ | CSC_05_HFOL_HPO4 | adsorption of |
| CIP_03_CaHCO3 | $Ca^{2+} + HCO_3^- \leftrightarrow CaHCO_3^+$ | CSC_06_HFOL_H2PO4 | phosphates onto |
| CIP_04_CaPO4 | $Ca^{2+} + PO_4^{3-} \leftrightarrow CaPO_4^-$ | CSC_07_HFOL_H3PO4 | $X_{HFO,L}$ |
| CIP_05_CaHPO4 | $Ca^{2+} + HPO_4^{2-} \leftrightarrow CaHPO_4$ | CSC_08_HFOL_H | Protonation of $X_{HFO,L}$ |
| CIP_06_CaH2PO4 | $Ca^{2+} + H_2PO_4^- \leftrightarrow CaH_2PO_4^+$ | | |
| CIP_07_FeOH | $Fe^{3+} + OH^- \leftrightarrow FeOH^{2+}$ | **5) HFO aging processes** | |
| CIP_08_FeOH2 | $FeOH^{2+} + OH^- \leftrightarrow Fe(OH)_2^+$ | HFO_1_aging_HFOH | $X_{HFO,H} \rightarrow X_{HFO,L}$ |
| CIP_09_FeOH3 | $Fe(OH)_2^+ + OH^- \leftrightarrow Fe(OH)_{3(aq)}$ | HFO_2_aging_HFOL | $X_{HFO,L} \rightarrow X_{HFO,old}$ |
| CIP_10_FeOH4 | $Fe(OH)_2^+ + 2OH^- \leftrightarrow Fe(OH)_4^-$ | HFO_3_aging_HFOH,b | $X_{HFO,H,b} \rightarrow X_{HFO,L,b}$ |
| CIP_11_FeHPO4 | $Fe^{3+} + HPO_4^{2-} \leftrightarrow FeHPO_4^+$ | HFO_4_aging_HFOL,b | $X_{HFO,L,b} \rightarrow X_{HFO,old}$ |
| CIP_12_FeH2PO4 | $Fe^{3+} + H_2PO_4^- \leftrightarrow FeH_2PO_4^{2+}$ | | |

constants (pKa) and their temperature correction coefficients are taken from the NIST database (National Institute of Standards and Technology (2001)).

The Davies equation is used for a non-iterative correction of ionic concentrations with ionic activities and ion pairing. This should ensure achievement of a pH error <5%, with an effluent ionic strength comprised between 0.001 and 0.1 mol L$^{-1}$, which correspond to weak industrial and all domestic wastewaters (Batstone et al., 2012).

The precipitation reactions are kinetically modelled following Koutsoukos et al. (1980) and Musvoto et al. (2000). To ensure good initial speciation of ionic species in the bulk and influent, concentrations are initialized to values obtained by species decomposition with the Phreeqc software (version 2.18.3, USGS, Reston, Virginia, USA) (Parkhurst et al., 1980) on the basis of experimental results of Szabo et al. (2008).

## 2.2. The hydrous ferric oxide model

The precipitation of amorphous hydrous ferric oxide (HFO, considered to be Fe(OH)$_{3(s)}$ by Smith et al. (2008)) provides a number of adsorption sites for ions on its surface, which allow both adsorption and co-precipitation of ions with HFO. The term of co-precipitation is defined by the International Union of pure and Applied Chemistry (IUPAC) as "the simultaneous precipitation of a normally soluble component with a macro-component from the same solution by the formation of mixed crystals, by adsorption, occlusion or mechanical entrapment" (McNaught and Wilkinson, 1997). The model concepts are developed on the basis of this definition, focussing only on phosphates adsorption and co-precipitation.

The model is based on the concept of reactive site density (named active site factor, ASF expressed as sites/mole of HFO), consisting of oxygen binding sites on HFO for which phosphate species and protons are competing. An equilibrium model has already been developed on this basis by Smith et al. (2008). The total number of available sites per unit of volume (SiteT in mol m$^{-3}$) is defined as the product of the mean number of active site factors of HFO (i$_{ASF,HFO}$) and the amount of precipitated HFO (X$_{HFO}$ in mol Fe L$^{-1}$). Each site has the ability to form bidentate and monodentate surface complexes with HPO$_4^{2-}$, H$_2$PO$_4^-$ and H$_3$PO$_4$ (MUSIC model, (Hiemstra and VanRiemsdijk, 1996)). Bidentate species means that phosphate species (H$_2$PO$_4^-$ or H$_3$PO$_4$) are bound to two sites owning two iron atoms. Four state variables are then introduced representing phosphate species or protons that are adsorbed on HFO: X$_{HFO,H}$, X$_{HFO,H_2PO_4}$, X$_{HFO,H_3PO_4}$, and X$_{HFO,HPO_4}$. These state variables are expressed in terms of mol Fe L$^{-1}$.

In the equilibrium model of Smith et al. (2008), each complexation reaction is associated with an equilibrium constant, which will define the proportion of each species adsorbed on HFO and their equilibrium with the bulk phase. These constants, as the i$_{ASF,HFO}$ were determined heuristically to describe the experimental data. The mean number of active site factors of HFO (i$_{ASF,HFO}$) has been found to depend on mixing intensity and HFO aging (Smith et al., 2008; Szabo et al., 2008), and should then be recalibrated for each experimental condition in this model. Furthermore this equilibrium model was not designed to describe the experimental results observed by Szabo et al. (2008), such as kinetic behaviour of

phosphorus removal consisting of an initial fast removal followed by slow removal, and the influence of HFO aging (loss of active surface sites).

Consequently, the kinetic model developed in this study aims to overcome these limitations. The equilibrium model developed by Smith et al. (2008) is retained and kinetic rates toward the equilibrium state are added. It results in one HFO precipitation process, four HFO aging processes and eight chemical surface complexation processes (4 complexation processes on X$_{HFO,H}$ and 4 complexation processes on X$_{HFO,L}$). These processes are described in more detail below and in a Gujer matrix (Appendix A and B) for the stoichiometry and kinetics, and schematically synthesized on Fig. 1. The model has been checked for continuity following the methodology described in Hauduc et al. (2010).

### 2.2.1. HFO precipitation

Rose and Waite (2003) and Pham et al. (2006) invoke a surface-mediated precipitation phenomenon for ferrihydrite, with a solubility product varying with the precipitate surface area, which would then not fit with the approach of Koutsoukos et al. (1980). Furthermore they found experimental evidence of a kinetic dependence on Fe(OH)$_{3(aq)}$ concentration, which would be the dominant precursor for polymerization of ferrihydrite. They propose first order kinetics with respect to total iron (Fe$_T$, dissolved and precipitated) and to the Fe(OH)$_{3(aq)}$ concentration. The approach of Rose and Waite (2003) was chosen in this study and presented in Equation (1).

$$Rate_{PMP_{HFO},pre} = q_{PMP_{HFO pre}} * S_{FeOH_3 aq} * Fe_T * \left( \frac{S_{FeOH_3 aq}}{S_{FeOH_3 aq} + 10^{-10}} \right) \qquad (1)$$

### 2.2.2. HFO aging

The ferrihydrite is considered to initially precipitate as X$_{HFO,H}$ with a high adsorption capacity, which will flocculate in larger aggregates. The floc growth depends on the mixing intensity (mean shear rate expressed as G value in s$^{-1}$), the concentration of metal and on the collision efficiency of the flocs (Duan and Gregory, 2003). Indeed, a limiting floc size exists at which collision efficiency decrease and disruptive forces increase and lead to floc breakage (Duan and Gregory, 2003).

This phenomenon is usually modelled as aggregation and breakage processes (Elimelech et al., 1995; Jarvis et al., 2005; Thomas et al., 1999) by a population mass balance. This complex problem may be approximated, for example by discretization (Vanni, 2000). The population of X$_{HFO}$ is then discretized into three classes: a HFO population with a high i$_{ASF,HFO}$ (X$_{HFO,H}$), a population with a low i$_{ASF,HFO}$ (X$_{HFO,L}$) and a population with no more adsorption capacity X$_{HFO,old}$. These three populations represent respectively: (1) fresh HFO with an open structure and easily accessible binding sites, (2) an older HFO type with a more compact structure and less accessible sites, which will be reached with a lower diffusion rate of ions, and (3) a very old population, which may be more crystallized. The related state variables are expressed in mol Fe L$^{-1}$, which is equivalent to the molar concentration of Fe(OH)$_{3(s)}$.

The aging mechanism leads to a loss of reactivity of the HFO, for which process the kinetic rate expression developed
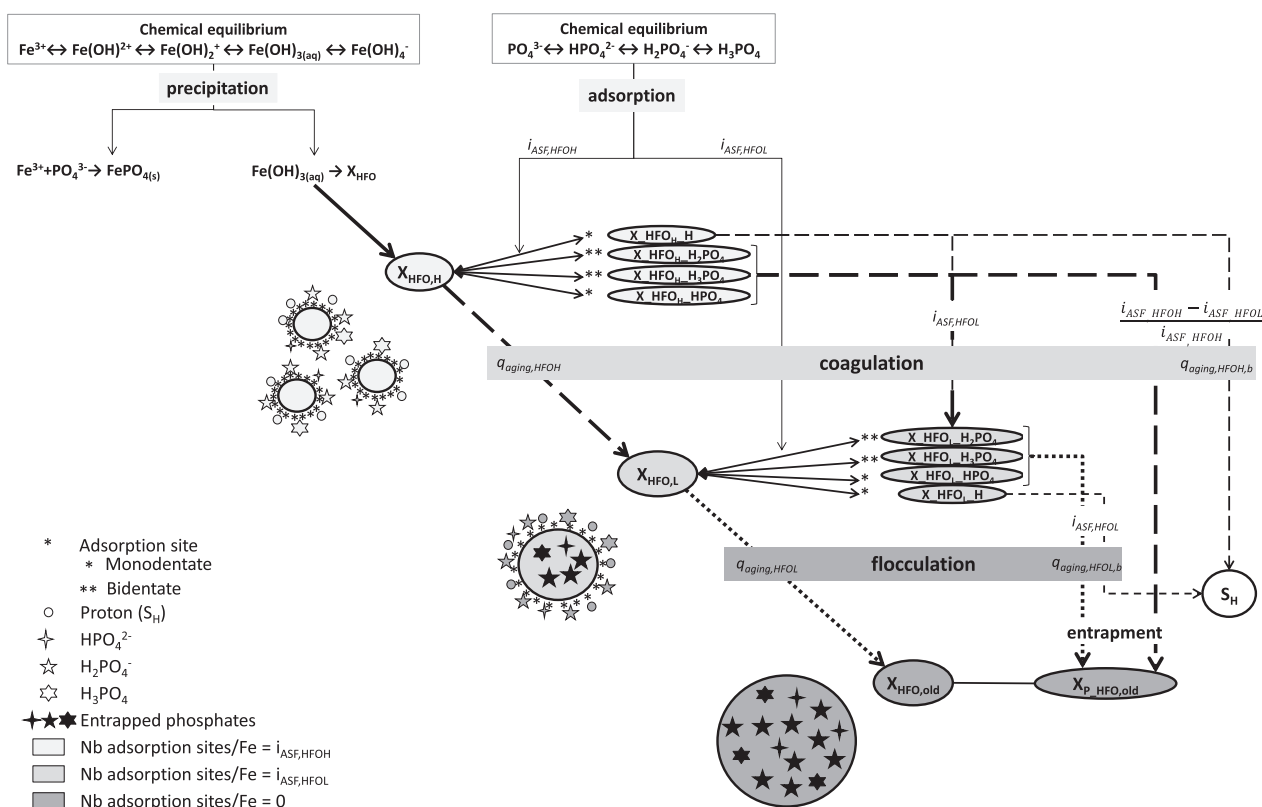
**Fig. 1 – Description of adsorption and co-precipitation of phosphate on HFO modelling concepts.**

by Bligh and Waite (2010) is chosen, with a general form presented in Equation (2), i being the considered population. As mentioned above, the coefficient $q_{aging}$ in this study depends on the mixing intensity (G value). The exact form of the dependence will be studied and commented in the results section.

$$\text{Rate} = q_{aging} * [X_{HFO,i}]^4 \big/ [X_{HFO\_T}]^2 \qquad (2)$$

As flocs become older and larger, the importance of floc breakage increases over aggregation, resulting in a lower overall rate of floc growth (Jarvis et al., 2005). A reduction factor $\eta_L$ is then introduced to lower the kinetic rate of $X_{HFO,L}$ aging compare to $X_{HFO,H}$ aging process. Furthermore, the formation of complexes seems to suppress the hydrolysis and polymerization processes of HFO precipitation, which leads to smaller ferrihydrite particles (Galvez et al., 1999; Karlsson and Persson, 2012). The aging kinetic rates are then considered to be different for bounded HFO and free HFO, and two reduction factors are introduced to lower the kinetic rates of $X_{HFOH,bT}$ (bounded $X_{HFO,H}$) and $X_{HFOL,bT}$ (bounded $X_{HFO,L}$) aging processes, respectively $\eta_{b,H}$ and $\eta_{b,L}$ (A). This results into four processes of HFO aging to describe the coagulation of bounded and free fresh HFO and then their flocculation, leading to old HFO structure with no reactive sites ($X_{HFO,old}$).

Lijklema (1980) shows that desorption of phosphates due to pH changes (increase) are not completely reversible, and even less if the HFO is older. This is considered by modelling simultaneously with coagulation and flocculation, the entrapment of phosphates that are already bounded on reactive sites into the structure of the HFO. These entrapped phosphates will not contribute to the equilibrium between adsorbed and free phosphates any more. Consequently the ratio P/Fe of the inactive HFO will evolve over time depending on the history of the HFO and its bounded phosphates. To count for entrapped phosphates, a state variable $X_{P\_HFO,old}$ expressed in mol P L$^{-1}$ is then introduced.

### 2.2.3. Phosphates adsorption onto HFO

The state variables $X_{HFOH\_H}$, $X_{HFOH\_H_2PO_4}$, $X_{HFOH\_H_3PO_4}$, and $X_{HFOH\_HPO_4}$ and their equivalent for $X_{HFOL}$ represent the ferrihydrite with bounded adsorption sites. They are expressed in term of mol Fe L$^{-1}$ and their equivalent proton or phosphate contents is calculated from their stoichiometry (bidentate or monodentate complexes) and the $i_{ASF,HFO}$ of the considered population (see continuity matrix of Appendix A).

The kinetic rate expressions for complexation processes are developed based on Lagergren's kinetic equation (Lagergren, 1898), in the same way as chemical equilibrium kinetic rate equations. This equation for the liquid/solid adsorption system expresses the variation of component concentrations as a function of a driving force, being the difference between the amounts of the component that should be bound at equilibrium of the system, calculated based on equilibrium constants and the actual bounded component. An order of the reaction of one with respect to the driving force for monodentate species and of two for bidentate species is considered, in accordance with Qiu et al. (2009). The

**Table 2 – Experimental condition of the selected datasets from Szabo et al. (2008).**

| Dataset | Corresponding figure | | Chemical condition | | | Physical conditions | | |
|---|---|---|---|---|---|---|---|---|
| # | This article | Szabo et al. (2008). | Fe/P dose [mol/mol] | $P_{ini}$ [mg L$^{-1}$] | pH | Mixing G [s$^{-1}$] | Aging [min] | Duration [min] |
| Calibration | | | | | | | | |
| 1 | Fig. 3 | Fig. 1 | 0.43–7.42 | 3.5 | 6.5 | 425 | – | 11 |
| 2 | Fig. 4 | Fig. 16 | 1.8 | 4.1 | 6.5 | 4–371 | – | 11 |
| 3 | Fig. 5 | Fig. 17 | 3 | 1 | 6.5 | 425 | 1–30 | 20 |
| Validation | | | | | | | | |
| 4 | Fig. 6 | Fig. 11 | 0.25–7 | 0.5–3 | 7 | 425 | – | 11 |
| 5 | Fig. 7 | Fig. 8 | 1.5–3 | 3.75 | 3.5–10 | 425 | – | 11 |
| 6 | Fig. 8 | Fig. 13 | 1–3 | 0–6 | 6.5 | 425 | – | 290 |
| 7 | Fig. 9 | Fig. 15 | 1 | 3 | 7.5 | 2–425 | – | 100 |

equilibrium constant determined experimentally by Antelo et al. (2010) for ferrihydrites are chosen as starting point.

The ferrihydrite flocs are porous and their adsorption sites are consequently not all equally accessible. Considering that the more accessible sites are bounded first, the subsequent decrease of the kinetic rate due to the decrease of accessibility of remaining sites have to be taken into account. A term $(SiteF/SiteT)^n$ is then introduced in the kinetic expression to moderate the kinetic constant, with n = 2 for bidentate species and n = 1 for monodentate species. This ratio represents the amount of free sites to the amount of total sites, its value being bounded between 0 and 1.

### 2.3. Model implementation and calibration

This model is implemented in Aquasim software (version 2.1g, EAWAG, Dübendorf, Switzerland) (Reichert, 1994).

The laboratory experiments from Szabo et al. (2008) provide a large number of results obtained under different conditions. These conditions may be categorized into two types: 1) the chemical conditions for which influence of iron dose, initial phosphorus concentration or pH have been tested; and 2) physical conditions for which influence of initial mixing intensity, aging processes (aggregation of flocs with time) and reaction duration (kinetic) have been investigated. Among the available results, three set of data have been chosen for calibration and four have been selected for validation of the model. The experimental conditions of these datasets are synthesized in Table 2.

The three datasets selected for calibration allow investigating all the experimental condition tested: Effect of dose and pH for dataset 1 (final pH being), effect of mixing for dataset 2 and effect of aging for dataset 3. The parameters considered in the model are listed in Table 3. As the uncertainties on the datasets cannot be evaluated (analytical uncertainties and sampling time), this calibration exercise does not aim to predict with accuracy all the values, but to determine a parameter set that describes all the selected datasets in order to validate the model structure. Each set of data leads to calibration of part of the parameters and the new parameter set is compared iteratively to other sets of data, as schematically represented in Fig. 2.

## 3. Results

### 3.1. Model calibration

The simulation of dataset #1 have reproduced the residual soluble phosphorus obtained after 11 minutes for different Fe/P ratio (0.43, 1.28, 2.54, 3.80 and 7.42) with initial pH of 6.5, initial phosphorus concentration of 3.5 mg L$^{-1}$ and initial alkalinity of 125 mg CaCO3 L$^{-1}$. The batch tests were performed first with a high stirring period of 1 minute at G = 425 s$^{-1}$, followed by a gentle stirring period of 10 minutes. The experimental results and simulation results are shown in Fig. 3.

**Table 3 – Model parameter values. Parameters in italic are not used in the simplified model.**

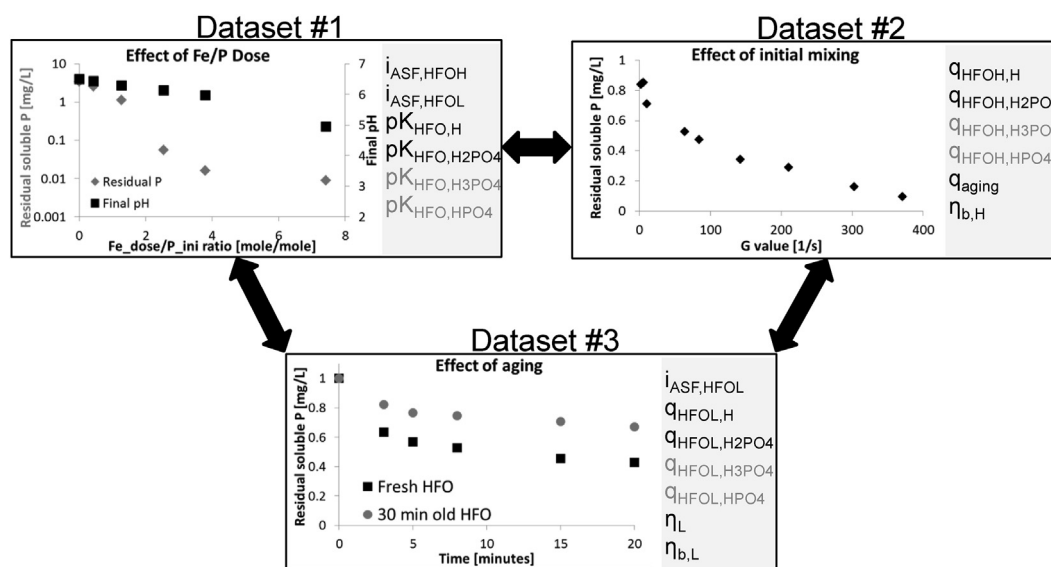| ASF values | | | Kinetic rate constants | | |
|---|---|---|---|---|---|
| $i_{ASF,HFOH}$ | 1.53 | Sites/mole of $X_{HFO\_H}$ | $q_{HFOH,H}$ | 1e$^{-5}$ | d$^{-1}$ |
| $i_{ASF,HFOL}$ | 0.63 | Sites/mole of $X_{HFO\_L}$ | $q_{HFOH,H_2PO_4}$, $q_{HFOH,H_3PO_4}$ | 1.5e$^{-6}$ | L mol$^{-1}$ d$^{-1}$ |
| | | | $q_{HFOH,HPO_4}$ | 5e$^{-4}$ | d$^{-1}$ |
| Equilibrium constants (pK values = −log K) | | | $q_{HFOL,H}$ | 5e$^{-6}$ | d$^{-1}$ |
| | Initial[a] | Calibrated | $q_{HFOL,H_2PO_4}$, $q_{HFOL,H_3PO_4}$ | 2e$^{-8}$ | L mol$^{-1}$ d$^{-1}$ |
| $pK_{HFO,H}$ | −8.7 | −8.7 | $q_{HFOL,HPO_4}$ | 5e$^{-5}$ | d$^{-1}$ |
| $pK_{HFO,H_2PO_4}$ | −8.157 | −8.193 | $q_{PMP,HFO,pre}$ | 1e$^{10}$ | L mol$^{-1}$ d$^{-1}$ |
| $pK_{HFO,H_3PO_4}$ | −10.339 | −10.334 | **Aging parameters** | | |
| $pK_{HFO,HPO_4}$ | −7.265 | −5.698 | $\eta_L$ | 2.5e$^{-4}$ | – |
| | | | $\eta_{b,H}$ | 1e$^{-5}$ | – |
| | | | $\eta_{b,L}$ | 0.4 | – |

[a] from Antelo et al. (2010).

Fig. 2 — Calibration procedure and parameters identified with each dataset. Parameters in grey are not used in the simplified model.

This set of experiments allows calibration of equilibrium constants and $i_{ASF,HFO}$ values (Table 3).

The simulation results are relatively close to experimental observations in terms of final phosphorus concentration with absolute percent errors between 4 and 32% (Table 4, left column). The final simulated pH values (squares on Fig. 3) are very close to the measured pH, with an error below 3%.

The previous batch tests were performed at high mixing intensity with a G value of 425 s$^{-1}$, which may not be the case at dosing point of wastewater treatment plants. For dataset #2 (Fig. 4), the influence of mixing intensity was investigated by Szabo et al. (2008) with 9 batch tests with varying intensity between 2 and 370 s$^{-1}$, which reveals lower removal capacity at lower G values after 10 minutes of reaction.

Because aging process depends on aggregation (coagulation and flocculation) which is influenced by mixing, a kinetic

constant $q_{aging}$ have been identified for each batch test and a function of G is calibrated on these values (Fig. 4 a). The determined expression is presented on Equation (3) and the associated simulation results are presented in Fig. 4b. The reduction factor $\eta_{b,H}$ to decrease the aging kinetic rate in case of bounded HFO is calibrated.

$$q_{aging} = 9.0e^7 \cdot \exp\left(-G/57.3\right) \tag{3}$$

The fitting of dataset #2 is very good for intermediate G value with an absolute percent error below 10% for G between
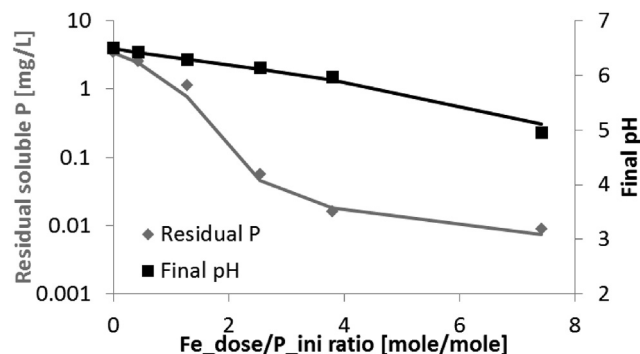


Fig. 3 — Dataset #1. Effect of initial Fe/P molar ratio on residual soluble phosphorus (diamonds) and on final pH (squares) of the batch: experimental results from Szabo et al. (2008) and simulation results (lines) (batch tests of 11 min, $P_{ini}$ = 3.5 mg L$^{-1}$, pH$_{ini}$ = 6.5, Alk$_{ini}$ = 125 mg CaCO$_3$ L$^{-1}$, G = 425 s$^{-1}$).

| Table 4 — Quality criteria of model adjustment with all the chemical surface complexation (CSC) processes considered, or considering only proton and $H_2PO_4^-$ chemical surface complexation processes. | | |
|---|---|---|
| Condition | Full model | Simplified model |
| Dataset#1 (Fig. 3) (Percent Error) | | |
| Fe/P = 0.43 | −4% | −4% |
| Fe/P = 1.28 | −32% | −31% |
| Fe/P = 2.54 | −20% | −19% |
| Fe/P = 3.80 | 12% | 13% |
| Fe/P = 7.42 | −27% | −18% |
| Dataset#2 (Fig. 4) (Percent Error) | | |
| G = 371 | 114% | 116% |
| G = 303 | 34% | 35% |
| G = 211 | −8% | −8% |
| G = 143 | 6% | 6% |
| G = 84 | 5% | 5% |
| G = 64 | 5% | 6% |
| G = 10 | 2% | 3% |
| G = 4 | −12% | −12% |
| Dataset#3 (Fig. 5) (Mean Percent Error) | | |
| 1 min old floc | −13% | −8% |
| 5 min old floc | 0% | 4% |
| 10 min old floc | −13% | −13% |
| 30 min old floc | 4% | 7% |

**Fig. 4 – Dataset #2. Effect of G value (mixing intensity) on a) the value of the aging constant calibrated and b) on residual soluble phosphorus: experimental results from Szabo et al. (2008) (diamonds) and simulation results (line) (batch tests of 11 min, $P_{ini}$ = 4.1 mg/L, $Fe/P_{ini}$ = 1.8 mole/mole).**

10 and 211 $s^{-1}$, slightly higher for G = 2 (12%) and 34% and 114% for respectively G = 303 and 371 $s^{-1}$ (Table 4, left column).

To analyse the influence of HFO age on removal capacity, Szabo et al. (2008) performed for dataset #3 a series of four batch tests where HFO are separately formed with a high initial stirring period of 1 minute at G = 425 $s^{-1}$ and added to the phosphorus solution after 1, 5, 10 or 30 minutes. For each batch two samples are taken at 3 and 20 minutes after HFO addition. The simulation results obtained are presented in Fig. 5.

This data set allows identification of the reduction factors for aging processes of unbounded and bounded $X_{HFO,L}$ (respectively $\eta_L$ and $\eta_{b,L}$), the phosphate adsorption rates on $X_{HFO,L}$ and the $i_{ASF, HFOL}$ value.

The simulated results show the same tendency as the experimental observation with a loss of removal capacity of the HFO after the same duration of contact with phosphorus solution. The adjustment of model to dataset is good, with a mean percent error below 13% for each condition (Table 4, left column).

### 3.2. Model simplifications

The simulations reveal that $FePO_4$ does not precipitate under the tested conditions. The simplification of the model by inactivating $FePO_4$ precipitation process and associated ion paring processes (CIP_11 and 12) leads to exactly the same results.

The analyse of dynamics of iron forms reveals that $Fe^{3+}$, $FeOH^{2+}$ and $Fe(OH)_4^-$ concentrations reach very low concentration in less than 1 minute due to precipitation. The model have then been simplified to keep only $Fe(OH)_2^+$ and $Fe(OH)_{3(aq)}$ processes to correctly describe the pH and the precipitation of HFO (disabling CIP_7, 8, and 10). This leads to exactly the same results.

In the test pH range the dominant adsorbed phosphate is $H_2PO_4^-$ which represents more than 95% of the adsorbed phosphates species. The model is then tested with enabling only CSC_2, 4, 6 and 8 processes ($H_2PO_4^-$ and $H^+$ adsorption). The quality criteria of model adjustment are presented in Table 4, right column and show very similar results than with model considering adsorption of all phosphate species. Consequently, only CSC_2, 4, 6 and 8 processes ($H_2PO_4^-$ and $H^+$ adsorption) may be considered.



**Fig. 5 – Dataset #3. Effect of HFO aging on residual soluble phosphorus: experimental results from Szabo et al. (2008) (points) and simulation results (lines). (batch tests with $P_{ini}$ = 1 mg/L and $Fe/P_{ini}$ = 3.0 mole/mole, addition of preformed hydrous ferric oxides after 1, 5, 10 and 30 minutes; samples at 3 and 20 minutes after ferric chloride solution addition).**



**Fig. 6 – Dataset #4. Effect of initial Fe/P ratio and initial P concentration on residual soluble phosphorus: experimental results from Szabo et al. (2008) (points) and simulation results (lines) (batch tests of 11 min).**
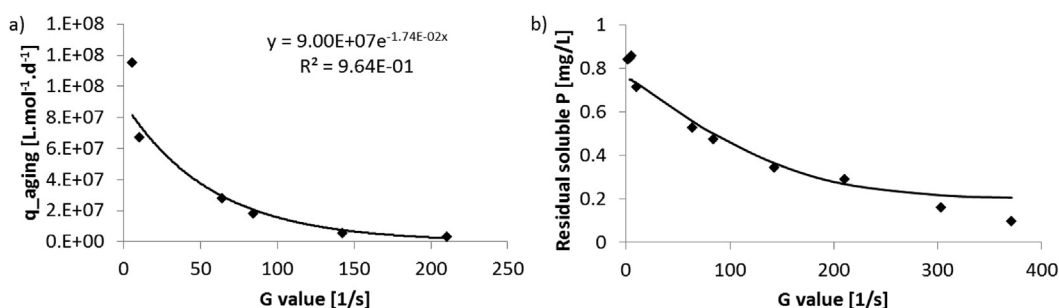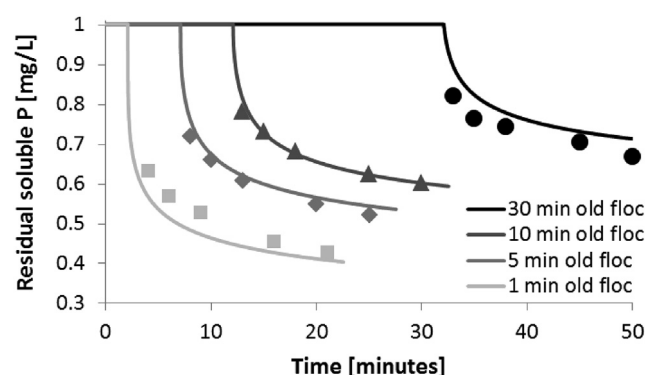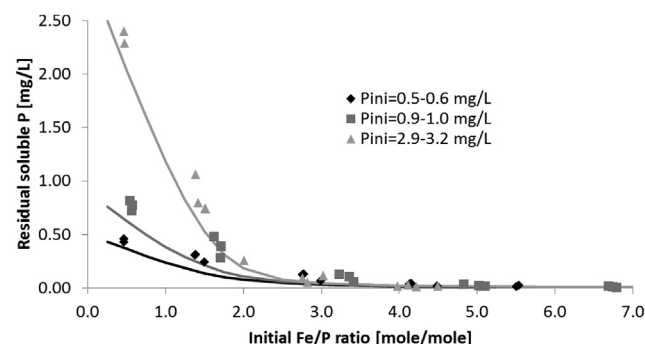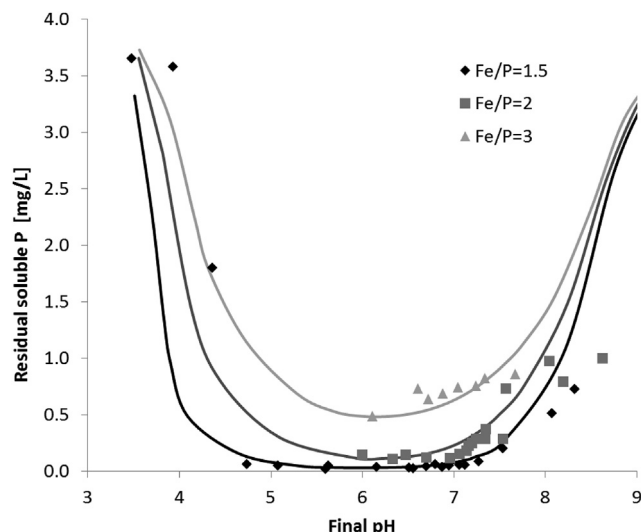
**Fig. 7 − Dataset #5. Effect of pH and initial Fe/P ratio on residual soluble phosphorus: experimental results from Szabo et al. (2008) (points) and simulation results (lines) (batch tests of 11 min, $P_{ini}$ = 3.75 mg/L).**

### 3.3. Model validation

The simplified model with determined parameter set is compared to independent datasets obtained under different conditions.

Datasets #4 and #5 (respectively represented on Fig. 6 and Fig. 7) allow validating the ability of the model to represent behaviour under different chemical conditions of initial phosphorus concentration, iron dose and pH. These datasets are globally well represented by the model, and the pH behaviour is well represented between pH 4.5 and 8 (Fig. 7).

Datasets #6 and #7 (respectively represented on Fig. 8 and Fig. 9) allow testing the ability of the model to simulate kinetic behaviour and the effect of various mixing conditions. The initial fast removal of phosphorus occurring in less than one minute (instantaneous phosphorus removal) is well represented for both datasets. However, the further removal (slow phosphorus removal) occurring in several hours is not accurately modelled, especially for dataset #6 (Fig. 8). The effect of the mixing intensity is well represented for G = 425 s$^{-1}$, less for G = 22.5 s$^{-1}$ and poorly for G = 2 s$^{-1}$.

## 4. Discussion

### 4.1. Prediction capabilities of the model

In this study the main operating parameters were considered through both chemical conditions (iron dose, initial phosphorus concentration or pH) and physical conditions (initial mixing intensity, aging processes due to aggregation of flocs with time and kinetic). For the first time a model is here proposed to describe the variation of adsorption capacity due simultaneously to precipitates aging, two different bounding sites capacities and entrapment.

The effect of Fe/P molar ratio is very well represented by all the simulations, either for simultaneous feeding or successive feeding thanks to the description of aging mechanism. Indeed the amount of phosphates removed by a given amount of iron will depend on the Fe/P dose, the initial phosphates concentration and on the number of adsorption sites which is related to floc size and depends on the age of the flocs and the mixing regime under which they have precipitated. In addition the model gives satisfying prediction for various residual phosphates concentrations from 0.01 to 3 mg P L$^{-1}$ and in the range of pH 4.5 to 8.

The calibration of dataset #1 leads to the calibration of $i_{ASF}$ values slightly higher than those determined by Smith et al. (2008) in the range of [0.2−1.18] Sites mol$^{-1}$. Those values should be confirmed with experiments under real activated sludge matrices, which organic matter may complex with HFO and leads to smaller ferrihydrite particles (Karlsson and Persson, 2012).

The loss of phosphate adsorption capacity of HFO flocs with time is well described by the model in a range of time from 5 to 30 minutes (Fig. 3). Effect of mixing intensity is also predicted by the model with satisfying results for G values in a range from 5 to 425 s$^{-1}$. The calibration of mixing intensity effect is very sensitive to parameter $\eta_{b,H}$, i.e. the reduction factor for the aging rate in case of bounded HFO (kinetic expression of HFO2 in A). This parameter allows a good spread of residual phosphorus values as function of G.

The $q_{aging}$ function has been fitted based on dataset #2 with initial phosphorus concentration of 4.1 mg/L. However the model seems to underestimate the aging process in the case of a G of 2 s$^{-1}$ in dataset #7, for which initial phosphorus was 1 mg/L. This is logical as the rate $q_{aging}$ was not correctly predicted for very low value of G with the exponential model
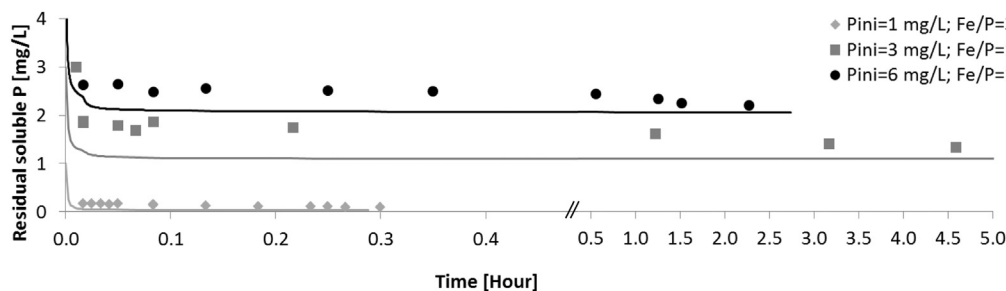


**Fig. 8 − Dataset #6. Effect of initial phosphorus concentration on kinetics of residual soluble phosphorus: experimental results from Szabo et al. (2008) (points) and simulation results (lines).**
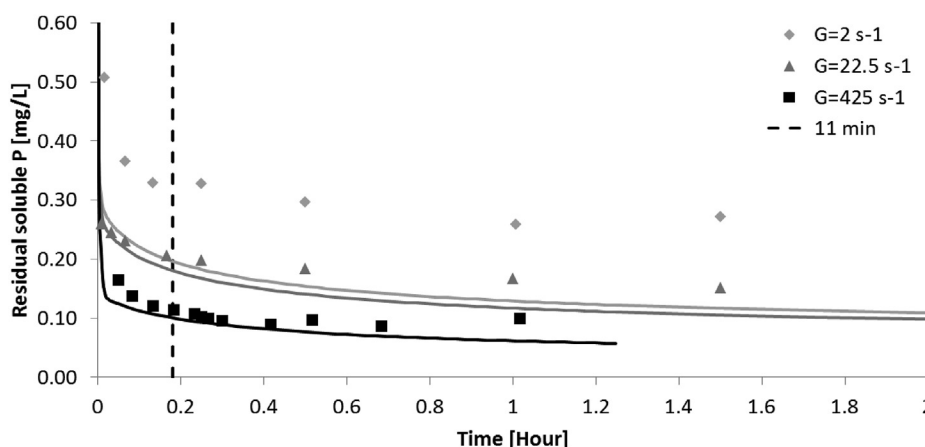
Fig. 9 – Dataset #7. Effect of initial mixing on kinetics of residual soluble phosphorus: experimental results from Szabo et al. (2008) (points) and simulation results (lines). (batch tests with $P_{ini} = 1$ mg/L and $Fe/P_{ini} = 3.0$ mole/mole).

chosen (Fig. 4). Such a very slow mixing is relatively extreme. Therefore, this kinetic model of aging should be compared with further experimental results and full-scale mixing conditions which may greatly differ from jar-test conditions.

### 4.2.  About model simplifications and further needs

The simulated amount of phosphorus precipitated in the form of $FePO_4$ is shown to be negligible ($<10-12$ mg P L$^{-1}$), which is consistent with the work of Smith et al. (2008) showing no $FePO_4$ precipitation above pH 5. This further indicates that the existing models based on precipitation in the form of $FePO_4$ are not suitable to describe the mechanisms observed.

The dominant simulated adsorbed phosphate is $H_2PO_4$ ($>95\%$ of the adsorbed phosphates species), which is consistent with experimental observations of Hiemstra and VanRiemsdijk (1996) who measured more than 85% of this surface species over pH range of 3.5–8. Antelo et al. (2010) shows no significant improvement in modelling $HPO_4^{2-}$ species adsorption onto HFO, whereas Rahnemaie et al. (2007) choose to neglect $H_3PO_4$ adsorption, since its concentration is negligible above pH 4. Furthermore, the equilibrium constant $pK_{HFO,HPO_4}$ (determined at $-5.698$ before simplification) takes a large range of values in literature, from 3.125 (Smith et al., 2008) to 15.255 (Rahnemaie et al., 2007). This reveals the uncertainty on this adsorption process. Consequently, the simplification of both $HPO_4^{2-}$ and $H_3PO_4$ adsorption onto HFO in this study is consistent with previous work. The simplification of $HPO_4^{2-}$ species by Antelo et al. (2010) leads the author to recalibrate the thermodynamic constant $pK_{HFO,H_2PO_4}$ from $-8.157$ to $-8.207$, which value is very close to the one determined in this study ($-8.193$).

The model validation step demonstrates the validity of the simplified model in the range of pH 4.5 to 8. In this range of pH the iron forms $Fe(OH)_4^-$ and $Fe(OH)_3$ are predominant, and thus sufficient to correctly predict the HFO precipitation. In this range of pH, $FePO_4$ precipitation is also negligible, just as the $H_3PO_4$ adsorption onto HFO. However $HPO_4^{2-}$ is one of the major phosphate ionic form in this range of pH (50% at pH 7.2

and major ionic for above). Consequently the simplifications made in this model by not considering its adsorption onto HFO do not depend only on the hypothesis made on the pH range applicability, but on the adsorption process itself. Indeed, Hiemstra and VanRiemsdijk (1996) specify that $HPO_4^{2-}$ species adsorption may become important at high pH and low P charge. The available datasets show the ability of the model to predict phosphates adsorption for initial phosphate concentration as low as 1 mg/L, but the applicability limit for lower initial phosphates concentration would require to be evaluated with additional experiments.

Above pH 7.5–8 the model results presented on Fig. 7 show significant differences with experimental data. At this pH other components of the tap water used for these experiments, such as calcium phosphate, may precipitate. This precipitates may have to be considered for model validation with real wastewater.

All the experimental observations revealed an initial fast removal of phosphorus occurring in less than one minute (instantaneous phosphorus removal), and a further removal (slow phosphorus removal) as observed by Szabo et al. (2008). The results demonstrate the ability of the model to correctly predict the initial fast removal process with aging but poorly the further slow removal. This behaviour of the model may be explained by the choice to represent the distribution of HFO flocs properties by only three classes ($X_{HFO,H}$, $X_{HFO,L}$ and $X_{HFO,old}$). The impact of this choice should be further investigated, especially in case of full scale results.

The calibration exercise on both influence of initial mixing rate and HFO aging evidenced a competition between adsorption and aging processes, to which parameters the model is very sensitive and impact both equilibrium and kinetic behaviour. Consequently, these processes should be carefully calibrated on full scale case study. At this stage it is not possible to say that the identification performed in this study will be directly applicable to full scale system. It is clear that the lab-scale conditions facilitate the homogeneity of the system. For industrial reactors performing such rapid processes a good

characterisation of hydrodynamics would be probably necessary in association with this model.

## 5. Conclusion

A new model has been developed to predict kinetically the precipitation of HFO, its aging processes and phosphates adsorption and co-precipitation mechanisms in the framework of chemical phosphorus removal in wastewater treatment plants. The simulation results showed that the structure of the model describes adequately the mechanisms of adsorption and co-precipitation of phosphates into/onto HFO and that the model is robust under various experimental conditions.

In this work, the model was validated with experiments carried out in tap water with low ammonium content and other component precipitations were not considered. For a validation with real wastewater, the physico-chemical model should be extended to take into account ammonia dissociation, calcium and magnesium ion pairing and precipitation processes. The influence of other parameters on chemical phosphate removal should also be investigated, such as the competition with carbonates, TSS and organics (COD). The next step will be to implement this model in an activated sludge model and compare the results to pilot or full scale data to validate it under continuous condition. The behaviour of ferric iron ($Fe^{3+}$) under anaerobic condition, and especially its reduction into ferrous iron ($Fe^{2+}$) should also be studied and included in the model.

The model developed and validated could then be used in full scale wastewater treatment plant models to optimize chemical dosing simultaneously while ensuring compliant effluent phosphorus concentration. Optimization parameters could include quantity of chemicals, frequency, location(s), mixing intensity and sludge age.

## Acknowledgements

## Appendix A. Stoichiometric and kinetic matrix of chemical surface complex formation processes. Processes in grey are not considered in the simplified model.

| Name | $S_{HPO4}$ | $S_{H2PO4}$ | $S_{H3PO4}$ | $S_H$ | $X_{HFOH}$ | $X_{HFOHH}$ | $X_{HFOHHPO4}$ | $X_{HFOHH2PO4}$ | $X_{HFOHH3PO4}$ | $X_{HFOL}$ | $X_{HFOLH}$ | $X_{HFOLHPO4}$ | $X_{HFOLH2PO4}$ | $X_{HFOLH3PO4}$ | $X_{HFOold}$ | $X_{PHFOold}$ |
|---|---|---|---|---|---|---|---|---|---|---|---|---|---|---|---|---|
| Units | $HPO_4^{2-}$ [mol P.L$^{-1}$] | $H_2PO_4^-$ [mol P.L$^{-1}$] | $H_3PO_4$ [mol P.L$^{-1}$] | $H^+$ [mol H.L$^{-1}$] | HFO (Fe(OH)$_3$(aq)) with high $i_{ASF_{HFO}}$ [mol Fe.L$^{-1}$] | Protonated $X_{HFOH}$ [mol Fe.L$^{-1}$] | $X_{HFOH}$ bounded with $HPO_4^{2-}$ [mol Fe.L$^{-1}$] | $X_{HFOH}$ bounded with $H_2PO_4^-$ [mol Fe.L$^{-1}$] | $X_{HFOH}$ bounded with $H_3PO_4$ [mol Fe.L$^{-1}$] | HFO (Fe(OH)$_3$(aq)) with low $i_{ASF_{HFO}}$ [mol Fe.L$^{-1}$] | Protonated $X_{HFOL}$ [mol Fe.L$^{-1}$] | $X_{HFOL}$ bounded with $HPO_4^{2-}$ [mol Fe.L$^{-1}$] | $X_{HFOL}$ bounded with $H_2PO_4^-$ [mol Fe.L$^{-1}$] | $X_{HFOL}$ bounded with $H_3PO_4$ [mol Fe.L$^{-1}$] | Inactive HFO (Fe(OH)$_3$(s)) [mol Fe.L$^{-1}$] | Phosphorus entrapped into HFO structure [mol P.L$^{-1}$] |
| | | | | | **$X_{HFOH,T}$** | | | | | **$X_{HFOL,T}$** | | | | | | |
| | | | | | **$X_{HFOHf,T}$** | | **$X_{HFOHb,T}$** | | | **$X_{HFOLf,T}$** | | **$X_{HFOLb,T}$** | | | | |
| CSC1 | $-i_{ASF_{HFOH}}$ | | | | $-1$ | | $1$ | | | | | | | | | |
| CSC2 | | $-i_{ASF_{HFOH}}/2$ | | | $-1$ | | | $1$ | | | | | | | | |
| CSC3 | | | $-i_{ASF_{HFOH}}/2$ | | $-1$ | | | | $1$ | | | | | | | |
| CSC4 | | | | $-i_{ASF_{HFOH}}$ | $-1$ | $1$ | | | | | | | | | | |
| CSC5 | $-i_{ASF_{HFOL}}$ | | | | | | | | | $-1$ | | $1$ | | | | |
| CSC6 | | $-i_{ASF_{HFOL}}/2$ | | | | | | | | $-1$ | | | $1$ | | | |
| CSC7 | | | $-i_{ASF_{HFOL}}/2$ | | | | | | | $-1$ | | | | $1$ | | |
| CSC8 | | | | $-i_{ASF_{HFOL}}$ | | | | | | $-1$ | $1$ | | | | | |
| **Continuity matrix** | | | | | | | | | | | | | | | | |
| P | $1$ | $1$ | $1$ | | | | $i_{ASF_{HFOH}}$ | $i_{ASF_{HFOH}}/2$ | $i_{ASF_{HFOH}}/2$ | | | $i_{ASF_{HFOL}}$ | $i_{ASF_{HFOL}}/2$ | $i_{ASF_{HFOL}}/2$ | | $1$ |
| Fe | | | | | $1$ | $1$ | $1$ | $1$ | $1$ | $1$ | $1$ | $1$ | $1$ | $1$ | $1$ | |
| H | | | | $1$ | $i_{ASF_{HFOH}}$ | | | | | $i_{ASF_{HFOL}}$ | | | | | | |

**Kinetic rate expressions**

| CSC1 | Adsorption of $S_{HPO4}$ on $X_{HFOH}$ | $q_{HFOH_{HPO4}} * \dfrac{SiteF_H}{SiteT_H + \varepsilon} * \left( 10^{-pK_{HFOH_{HPO4}}} * S_{HPO4} * f_d * \dfrac{SiteF_H}{SiteT_H + \varepsilon} - i_{ASF_{HFOH}} * \dfrac{X_{HFOH_{HPO4}}}{SiteT_H} \right)$ |
|---|---|---|
| CSC2 | Adsorption of $S_{H2PO4}$ on $X_{HFOH}$ | $q_{HFOH_{H2PO4}} * \left( \dfrac{SiteF_H}{SiteT_H + \varepsilon} \right)^2 * \left( 10^{-pK_{HFOH_{H2PO4}}} * S_{H2PO4} * f_m * \left( \dfrac{SiteF_H}{SiteT_H + \varepsilon} \right)^2 - \dfrac{i_{ASF_{HFOH}} * X_{HFOH_{H2PO4}}}{SiteT_H + \varepsilon} \right)^2$ |
| CSC3 | Adsorption of $S_{H3PO4}$ on $X_{HFOH}$ | $q_{HFOH_{H3PO4}} * \left( \dfrac{SiteF_H}{SiteT_H + \varepsilon} \right)^2 * \left( 10^{-pK_{HFOH_{H3PO4}}} * S_{H3PO4} * f_m * \left( \dfrac{SiteF_H}{SiteT_H + \varepsilon} \right)^2 - \dfrac{i_{ASF_{HFOH}} * X_{HFOH_{H3PO4}}}{SiteT_H + \varepsilon} \right)^2$ |
| CSC4 | Adsorption of $S_H$ on $X_{HFOH}$ | $q_{HFOH_H} * \dfrac{SiteF_H}{SiteT_H + \varepsilon} * \left( 10^{-pK_{HFOH}} * S_H * f_m * \dfrac{SiteF_H}{SiteT_H + \varepsilon} - i_{ASF_{HFOH}} * \dfrac{X_{HFOH_H}}{SiteT_H + \varepsilon} \right)$ |
| CSC5 | Adsorption of $S_{HPO4}$ on $X_{HFOL}$ | $q_{HFOL_{HPO4}} * \dfrac{SiteF_L}{SiteT_L + \varepsilon} * \left( 10^{-pK_{HFOL_{HPO4}}} * S_{HPO4} * f_d * \dfrac{SiteF_L}{SiteT_L + e} - i_{ASF_{HFOL}} * \dfrac{X_{HFOL_{HPO4}}}{SiteT_L + e} \right)$ |
| CSC6 | Adsorption of $S_{H2PO4}$ on $X_{HFOL}$ | $q_{HFOL_{H2PO4}} * \left( \dfrac{SiteF_L}{SiteT_L + \varepsilon} \right)^2 * \left( 10^{-pK_{HFOL_{H2PO4}}} * S_{H2PO4} * f_m * \left( \dfrac{SiteF_L}{SiteT_L + \varepsilon} \right)^2 - \dfrac{i_{ASF_{HFOL}} * X_{HFOL_{H2PO4}}}{SiteT_L + \varepsilon} \right)^2$ |
| CSC7 | Adsorption of $S_{H3PO4}$ on $X_{HFOL}$ | $q_{HFOL_{H3PO4}} * \left( \dfrac{SiteF_L}{SiteT_L + \varepsilon} \right)^2 * \left( 10^{-pK_{HFOL_{H3PO4}}} * S_{H3PO4} * f_m * \left( \dfrac{SiteF_L}{SiteT_L + \varepsilon} \right)^2 - \dfrac{i_{ASF_{HFOL}} * X_{HFOL_{H3PO4}}}{SiteT_L + \varepsilon} \right)^2$ |
| CSC8 | Adsorption of $S_H$ on $X_{HFOL}$ | $q_{HFOL_H} * \dfrac{SiteF_L}{SiteT_L + \varepsilon} * \left( 10^{-pK_{HFOH}} * S_H * f_m * \dfrac{SiteF_L}{SiteT_L + \varepsilon} - i_{ASF_{HFOL}} * \dfrac{X_{HFOL_H}}{SiteT_L + \varepsilon} \right)$ |

## Appendix B. Stoichiometric and kineticmatrix of HFO aging processes.

| Name | $S_H$ | $X_{HFOH}$ | $X_{HFOH_H}$ | $X_{HFOH_{HPO4}}$ | $X_{HFOH_{H2PO4}}$ | $X_{HFOH_{H3PO4}}$ | $X_{HFOL}$ | $X_{HFOL_H}$ | $X_{HFOL_{HPO4}}$ | $X_{HFOL_{H2PO4}}$ | $X_{HFOL_{H3PO4}}$ | $X_{HFO_{old}}$ | $X_{P_{HFO_{old}}}$ |
|---|---|---|---|---|---|---|---|---|---|---|---|---|---|
| HFO1 | A | $\frac{-X_{HFOH}}{X_{HFOHf_T}+\varepsilon}$ | $\frac{-X_{HFOH_H}}{X_{HFOHf_T}+\varepsilon}$ | | | | $\frac{X_{HFOH}}{X_{HFOHf_T}+\varepsilon}$ | $\frac{X_{HFOH_H}}{X_{HFOHf_T}+\varepsilon}$ | | | | | |
| HFO2 | B | | | | | | $\frac{-X_{HFOL}}{X_{HFOLf_T}+\varepsilon}$ | $\frac{-X_{HFOL_H}}{X_{HFOLf_T}+\varepsilon}$ | | | | $\frac{X_{HFOL}+X_{HFOL_H}}{X_{HFOLf_T}+\varepsilon}$ | |
| HFO3 | | | | $\frac{-X_{HFOH_{HPO4}}}{X_{HFOHb_T}+\varepsilon}$ | $\frac{-X_{HFOH_{H2PO4}}}{X_{HFOHb_T}+\varepsilon}$ | $\frac{-X_{HFOH_{H3PO4}}}{X_{HFOHb_T}+\varepsilon}$ | | | $\frac{X_{HFOH_{HPO4}}}{X_{HFOHb_T}+\varepsilon}$ | $\frac{X_{HFOH_{H2PO4}}}{X_{HFOHb_T}+\varepsilon}$ | $\frac{X_{HFOH_{H3PO4}}}{X_{HFOHb_T}+\varepsilon}$ | | C |
| HFO4 | | | | | | | | | $\frac{-X_{HFOL_{HPO4}}}{X_{HFOLb_T}+\varepsilon}$ | $\frac{-X_{HFOL_{H2PO4}}}{X_{HFOLb_T}+\varepsilon}$ | $\frac{-X_{HFOL_{H3PO4}}}{X_{HFOLb_T}+\varepsilon}$ | D | E |

with

$$A=\left(\frac{i_{ASF_{HFOH}}-i_{ASF_{HFOL}}}{i_{ASF_{HFOH}}}*\left(i_{ASF_{HFOH}}*\frac{X_{HFOH_H}}{X_{HFOHf_T}+\varepsilon}\right)\right)$$

$$B=\left(i_{ASF_{HFOL}}*\frac{X_{HFOL_H}}{X_{HFOLf_T}+\varepsilon}\right)$$

$$C=\left(\frac{i_{ASF_{HFOH}}-i_{ASF_{HFOL}}}{i_{ASF_{HFOH}}}*\frac{(i_{ASF_{HFOL}}/2)*X_{HFOH_{H2PO4}}+(i_{ASF_{HFOL}}/2)*X_{HFOH_{H3PO4}}+i_{ASF_{HFOH}}*X_{HFOH_{HPO4}}}{X_{HFOHb_T}+\varepsilon}\right)$$

$$D=\frac{X_{HFOL_{H2PO4}}+X_{HFOL_{H3PO4}}+X_{HFOL_{HPO4}}}{X_{HFOLb_T}+\varepsilon}$$

$$E=\frac{(i_{ASF_{HFOL}}/2)*X_{HFOL_{H2PO4}}+(i_{ASF_{HFOL}}/2)*X_{HFOL_{H3PO4}}+i_{ASF_{HFOL}}*X_{HFOL_{HPO4}}}{X_{HFOLb_T}+\varepsilon}$$

**Kinetic rate expressions**

| | | |
|---|---|---|
| HFO1 | Aging of $X_{HFOH,fT}$ (unbounded $X_{HFOH}$) | $q_{aging}*X_{HFOHf_T}*\dfrac{X_{HFOH_T}^3}{X_{HFO_T}^2+\varepsilon}$ |
| HFO2 | Aging of $X_{HFOL,fT}$ (unbounded $X_{HFOL}$) | $\eta_L*q_{aging}*X_{HFOLf_T}*\dfrac{X_{HFOL_T}^3}{X_{HFO_T}^2+\varepsilon}$ |
| HFO3 | Aging of $X_{HFOH,bT}$ (bounded $X_{HFOH}$) | $\eta_{b,H}*q_{aging}*X_{HFOHb_T}*\dfrac{X_{HFOH_T}^3}{X_{HFO_T}^2+\varepsilon}$ |
| HFO4 | Aging of $X_{HFOL,bT}$ (bounded $X_{HFOL}$) | $\eta_L*\eta_{b,L}*q_{aging}*X_{HFOLb_T}*\dfrac{X_{HFOL_T}^3}{X_{HFO_T}^2+\varepsilon}$ |

## Appendix C. List of calculated variables.

| Name | Expression | Units |
|---|---|---|
| $SiteT_H$ | $(X_{HFOH}+X_{HFOH_H}+X_{HFOH_{H_2PO_4}}+X_{HFOH_{H_3PO_4}}+X_{HFOH_{HPO_4}})*i_{ASF_{HFOH}}$ | mol sites $L^{-1}$ |
| $SiteT_L$ | $(X_{HFOL}+X_{HFOL_H}+X_{HFOL_{H_2PO_4}}+X_{HFOL_{H_3PO_4}}+X_{HFOL_{HPO_4}})*i_{ASF_{HFOL}}$ | mol sites $L^{-1}$ |
| $SiteF_H$ | $(X_{HFOH}+X_{HFOH_H})*i_{ASF_{HFOH}}$ | mol sites $L^{-1}$ |
| $SiteF_L$ | $(X_{HFOL}+X_{HFOL_H})*i_{ASF_{HFOL}}$ | mol sites $L^{-1}$ |
| $Fe_T$ | $S_{FeT}+X_{HFOH_T}+X_{HFOH_T}$ | mol Fe $L^{-1}$ |
| $\varepsilon$ | Small number to avoid numerical problems with fractions ($10^{-16}$) | — |
| $f_m, f_d$ | Correction factors for ionic activities of mono- and divalent ions using Davies equation | — |

## Appendix D. Physico-chemical model.

**Table D.1 – Stoichiometric and kinetic matrix of chemical equilibrium dissociation, chemical ion paring and physical mineral precipitation processes. Processes in grey are not considered in the simplified model.**

| Name [Units] | $S_{CaCO3aq}$ | $S_{CaH2PO4}$ | $S_{CaHCO3}$ | $S_{CaHPO4}$ | $S_{CaOH}$ | $S_{CaPO4}$ | $S_{Ca}$ | $S_{CO3}$ | $S_{FeH2PO4}$ | $S_{FeHPO4}$ | $S_{FeOH2}$ | $S_{FeOH3aq}$ | $S_{FeOH4}$ | $S_{FeOH}$ | $S_{Fe}$ | $S_{H2CO3}$ | $S_{H2PO4}$ | $S_{H3PO4}$ | $S_{HCO3}$ | $S_{HPO4}$ | $S_{H}$ | $S_{OH}$ | $S_{PO4}$ | $X_{FePO4}$ | $X_{HFOH}$ |
|---|---|---|---|---|---|---|---|---|---|---|---|---|---|---|---|---|---|---|---|---|---|---|---|---|---|
| CED_01 | | | | | | | | | | | | | | | | | | | | | 1 | 1 | | | |
| CED_02 | | | | | | | | | | | | | | | | -1 | | | 1 | | 1 | | | | |
| CED_03 | | | | | | | | 1 | | | | | | | | | | | -1 | | 1 | | | | |
| CED_04 | | | | | | | | | | | | | | | | | 1 | -1 | | | 1 | | | | |
| CED_05 | | | | | | | | | | | | | | | | | -1 | | | 1 | 1 | | | | |
| CED_06 | | | | | | | | | | | | | | | | | | | | -1 | 1 | | 1 | | |
| CIP_01 | | | | | 1 | | -1 | | | | | | | | | | | | | | | -1 | | | |
| CIP_02 | 1 | | | | | | -1 | -1 | | | | | | | | | | | | | | | | | |
| CIP_03 | | | 1 | | | | -1 | | | | | | | | | | | | -1 | | | | | | |
| CIP_04 | | | | | | 1 | -1 | | | | | | | | | | | | | | | | -1 | | |
| CIP_05 | | | | 1 | | | -1 | | | | | | | | | | | | | -1 | | | | | |
| CIP_06 | | 1 | | | | | -1 | | | | | | | | | | -1 | | | | | | | | |
| CIP_07 | | | | | | | | | | | | | | 1 | -1 | | | | | | | -1 | | | |
| CIP_08 | | | | | | | | | | | 1 | | | -1 | | | | | | | | -1 | | | |
| CIP_09 | | | | | | | | | | | -1 | 1 | | | | | | | | | | -1 | | | |
| CIP_10 | | | | | | | | | | | | -1 | 1 | | | | | | | | | -1 | | | |
| CIP_11 | | | | | | | | | | 1 | | | | | -1 | | | | | -1 | | | | | |
| CIP_12 | | | | | | | | | 1 | | | | | | -1 | | -1 | | | | | | | | |
| PMP_1 | | | | | | | | | | | | -1 | | | | | | | | | | | | | 1 |
| PMP_2 | | | | | | | | | | | | | | | -1 | | | | | | | | -1 | 1 | |

**Kinetic rate expressions**

| | |
|---|---|
| **CED_01_H2O** | $q_{CED_{H2O}} * \left(10^{-pK_{CED_{H2O}}} * (1/f_m^2) - S_{OH} * S_H\right)$ |
| **CED_02_H2CO3** | $q_{CED_{H2CO3}} * \left(10^{-pK_{CED_{H2CO3}}} * (1/f_m^2) * S_{H2CO3} - S_H * S_{HCO3}\right)$ |
| **CED_03_HCO3** | $q_{CED_{HCO3}} * \left(10^{-pK_{CED_{HCO3}}} * (1/f_d) * S_{HCO3} - S_H * S_{CO3}\right)$ |
| **CED_04_H3PO4** | $q_{CED_{H3PO4}} * \left(10^{-pK_{CED_{H3PO4}}} * (1/f_m^2) * S_{H3PO4} - S_H * S_{H2PO4}\right)$ |
| **CED_05_H2PO4** | $q_{CED_{H2PO4}} * \left(10^{-pK_{CED_{H2PO4}}} * (1/f_d) * S_{H2PO4} - S_H * S_{HPO4}\right)$ |
| **CED_06_HPO4** | $q_{CED_{HPO4}} * \left(10^{-pK_{CED_{HPO4}}} * (f_d/(f_t * f_m)) * S_{HPO4} - S_H * S_{PO4}\right)$ |
| **CIP_01_CaOH** | $q_{CIP_{CaOH}} * \left(10^{-pK_{CIP_{CaOH}}} * f_d * S_{Ca} * S_{OH} - S_{CaOH}\right)$ |
| **CIP_02_CaCO3** | $q_{CIP_{CaCO3}} * \left(10^{-pK_{CIP_{CaCO3}}} * f_d^2 * S_{Ca} * S_{CO3} - S_{CaCO3aq}\right)$ |
| **CIP_03_CaHCO3** | $q_{CIP_{CaHCO3}} * \left(10^{-pK_{CIP_{CaHCO3}}} * f_d * S_{Ca} * S_{HCO3} - S_{CaHCO3}\right)$ |
| **CIP_04_CaPO4** | $q_{CIP_{CaPO4}} * \left(10^{-pK_{CIP_{CaPO4}}} * (f_d * f_t/f_m) * S_{Ca} * S_{PO4} - S_{CaPO4}\right)$ |
| **CIP_05_CaHPO4** | $q_{CIP_{CaHPO4}} * \left(10^{-pK_{CIP_{CaHPO4}}} * (f_d^2) * S_{Ca} * S_{HPO4} - S_{CaHPO4}\right)$ |
| **CIP_06_CaH2PO4** | $q_{CIP_{CaH2PO4}} * \left(10^{-pK_{CIP_{CaH2PO4}}} * f_d * S_{Ca} * S_{H2PO4} - S_{CaH2PO4}\right)$ |
| **CIP_07_FeOH** | $q_{CIP_{FeOH}} * \left(10^{-pK_{CIP_{FeOH}}} * (f_t * f_m/f_d) * S_{Fe} * S_{OH} - S_{FeOH}\right)$ |
| **CIP_08_FeOH2** | $q_{CIP_{FeOH2}} * \left(10^{-pK_{CIP_{FeOH2}}} * f_d * S_{FeOH} * S_{OH} - S_{FeOH2}\right)$ |
| **CIP_09_FeOH3** | $q_{CIP_{FeOH3}} * \left(10^{-pK_{CIP_{FeOH3}}} * f_m^2 * S_{FeOH2} * S_{OH} - S_{FeOH3aq}\right)$ |
| **CIP_10_FeOH4** | $q_{CIP_{FeOH4}} * \left(10^{-pK_{CIP_{FeOH4}}} * S_{FeOH3aq} * S_{OH} - S_{FeOH4}\right)$ |
| **CIP_11_FeHPO4** | $q_{CIP_{FeHPO4}} * \left(10^{-pK_{CIP_{FeHPO4}}} * (f_t * f_d/f_m) * S_{HPO4} * S_{Fe} - S_{FeHPO4}\right)$ |
| **CIP_12_FeH2PO4** | $q_{CIP_{FeH2PO4}} * \left(10^{-pK_{CIP_{FeH2PO4}}} * (f_t * f_m/f_d) * S_{H2PO4} * S_{Fe} - S_{FeH2PO4}\right)$ |
| **PMP_1_HFO_pre** | $q_{PMP_{HFOpre}} * S_{FeOH3aq} * FeT * \left(\dfrac{S_{FeOH3aq}}{S_{FeOH3aq} + \varepsilon}\right)$ |
| **PMP_2_FePO4** | $q_{PMP_{FePO4pre}} * \left((f_t^2 * S_{Fe} * S_{PO4})^{\frac{1}{2}} - (10^{-pK_{PMP_{FePO4}}})^{\frac{1}{2}}\right)^2$ |

**Table D.2 – Physico-chemical model parameter values.**

Equilibrium constants (pK values = −log K) corrected with temperature (from NIST 2001 database): $-log(10^{-pK_{25°C}} * exp(-\Delta/R*(1/T - 1/298.15)))$

Kinetic rate constants (from Musvoto et al. (2000))

| | pK (25 °C) | $\Delta$ (kJ mol$^{-1}$) | | (L mol$^{-1}$ d$^{-1}$) |
|---|---|---|---|---|
| pK_CED_H$_2$CO$_3$ | 6.352 | 9.16 | q_CED_H$_2$CO$_3$ | 8.64E + 11 |
| pK_CED_H$_2$O | 13.997 | 55.81 | q_CED_H$_2$O | 8.64E + 14 |
| pK_CED_H$_2$PO$_4$ | 7.198 | 3 | q_CED_H$_2$PO$_4$ | 8.64E + 16 |
| pK_CED_H$_3$PO$_4$ | 2.148 | −7.9 | q_CED_H$_3$PO$_4$ | 8.64E + 12 |
| pK_CED_HCO$_3$ | 10.329 | 14.6 | q_CED_HCO$_3$ | 8.64E + 14 |
| pK_CED_HPO$_4$ | 12.375 | 15 | q_CED_HPO$_4$ | 8.64E + 19 |
| pK_CIP_CaCO$_3$ | −3.2 | 16 | q_CIP_CaCO$_3$ | 8.64E + 11 |
| pK_CIP_CaH$_2$PO$_4$ | −1.35 | −24 | q_CIP_CaH$_2$PO$_4$ | 8.64E + 11 |
| pK_CIP_CaHCO$_3$ | −1.27 | −9.2 | q_CIP_CaHCO$_3$ | 8.64E + 11 |
| pK_CIP_CaHPO$_4$ | −2.66 | −18 | q_CIP_CaHPO$_4$ | 8.64E + 11 |
| pK_CIP_CaOH | −1.3 | 8.3 | q_CIP_CaOH | 8.64E + 11 |
| pK_CIP_CaPO$_4$ | −6.46 | 12.9704 | q_CIP_CaPO$_4$ | 8.64E + 11 |
| pK_CIP_FeH$_2$PO$_4$ | −4.2785 | −12.6 | q_CIP_FeH$_2$PO$_4$ | 8.64E + 11 |
| pK_CIP_FeHPO$_4$ | −9.917 | −45.5432 | q_CIP_FeHPO$_4$ | 8.64E + 11 |

**Table D.2 – (continued)**

| Equilibrium constants (pK values = −log K) corrected with temperature (from NIST 2001 database): $-log(10^{-pK_{25°C}}*exp(-\Delta/R*(1/T - 1/298.15)))$ | | | Kinetic rate constants (from Musvoto et al. (2000)) | |
|---|---|---|---|---|
| | pK (25 °C) | $\Delta$ (kJ mol$^{-1}$) | | (L mol$^{-1}$ d$^{-1}$) |
| pK_CIP_FeOH | −11.81 | −14 | q_CIP_FeOH | 8.64E + 11 |
| pK_CIP_FeOH$_2$ | −11.59 | −41.81 | q_CIP_FeOH$_2$ | 8.64E + 11 |
| pK_CIP_FeOH$_3$ | −6.031 | −184.994 | q_CIP_FeOH$_3$ | 8.64E + 11 |
| pK_CIP_FeOH$_4$ | −4.969 | −167.43 | q_CIP_FeOH$_4$ | 8.64E + 11 |
| Equilibrium constants for precipitation processes (pK values = −log K) | | | Kinetic rate constants for precipitation processes (Calibrated) | |
| pK_PMP_FePO$_4$ | 26.4 | Smith et al., 2008 (I = 0.02 M) | q_PMP_FePO$_4$_pre | 100,000 |
| pK_PMP_HFO | 15.4 | Smith et al., 2008 (I = 0.02 M) | q_PMP_HFO_pre | 1E + 10 |

## REFERENCES

Antelo, J., Fiol, S., Perez, C., Marino, S., Arce, F., Gondar, D., Lopez, R., 2010. Analysis of phosphate adsorption onto ferrihydrite using the CD-MUSIC model. J. Colloid Interface Sci. 347, 112–119. http://dx.doi.org/10.1016/j.jcis.2010.03.020.

Batstone, D.J., Amerlinck, Y., Ekama, G., Goel, R., Grau, P., Johnson, B., Kaya, I., Steyer, J.-P., Tait, S., Takács, I., Vanrolleghem, P.A., Brouckaert, C.J., Volcke, E., 2012. Towards a generalized physicochemical framework. Water Sci. Technol. 66, 1147–1161. http://dx.doi.org/10.2166/wst.2012.300.

Bligh, M.W., Waite, T.D., 2010. Formation, aggregation and reactivity of amorphous ferric oxyhydroxides on dissociation of Fe(III)-organic complexes in dilute aqueous suspensions. Geochim. Cosmochim. Acta 74, 5746–5762. http://dx.doi.org/10.1016/j.gca.2010.07.008.

Caravelli, A.H., Contreras, E.M., Zaritzky, N.E., 2010. Phosphorous removal in batch systems using ferric chloride in the presence of activated sludges. J. Hazard. Mater. 177, 199–208. http://dx.doi.org/10.1016/j.jhazmat.2009.12.018.

Corominas, L., Rieger, L., Takács, I., Ekama, G., Hauduc, H., Vanrolleghem, P.A., Oehmen, A., Gernaey, K.V., Comeau, Y., 2010. New framework for standardized notation in wastewater treatment modelling. Water Sci. Technol. 61, 841–857.

Duan, J.M., Gregory, J., 2003. Coagulation by hydrolysing metal salts. Adv. Colloid Interface Sci. 100, 475–502. http://dx.doi.org/10.1016/S0001-8686(02)00067-2.

Elimelech, M., Gregory, J., Jia, X., Williams, R.A., Gregory, J., Jia, X., Williams, R.A., 1995. Chapter 6-Modelling of aggregation processes. In: Particle Deposition & Aggregation. Butterworth-Heinemann, Woburn, pp. 157–202.

Fytianos, K., Voudrias, E., Raikos, N., 1998. Modelling of phosphorus removal from aqueous and wastewater samples using ferric iron. Environ. Pollut. 101, 123–130. http://dx.doi.org/10.1016/S0269-7491(98)00007-4.

Galvez, N., Barron, V., Torrent, J., 1999. Effect of phosphate on the crystallization of hematite, goethite, and lepidocrocite from ferrihydrite. Clays Clay Min. 47, 304–311. http://dx.doi.org/10.1346/CCMN.1999.0470306.

Hauduc, H., Rieger, L., Takács, I., Heduit, A., Vanrolleghem, P.A., Gillot, S., 2010. A systematic approach for model verification: application on seven published activated sludge models. Water Sci. Technol. 61, 825–839.

Hiemstra, T., VanRiemsdijk, W.H., 1996. A surface structural approach to ion adsorption: the charge distribution (CD) model. J. Colloid Interface Sci. 179, 488–508. http://dx.doi.org/10.1006/jcis.1996.0242.

Jarvis, P., Jefferson, B., Gregory, J., Parsons, S.A., 2005. A review of floc strength and breakage. Water Res. 39, 3121–3137. http://dx.doi.org/10.1016/j.watres.2005.05.022.

Karlsson, T., Persson, P., 2012. Complexes with aquatic organic matter suppress hydrolysis and precipitation of Fe(III). Chem. Geol. 322, 19–27. http://dx.doi.org/10.1016/j.chemgeo.2012.06.003.

Koutsoukos, P., Amjad, Z., Tomson, M.B., Nancollas, G.H., 1980. Crystallization of calcium phosphates. A constant composition study. J. Am. Chem. Soc. 102, 1553–1557. http://dx.doi.org/10.1021/ja00525a015.

Lagergren, S., 1898. About the theory of so-called adsorption of soluble substances. K. Sven. Vetenskapsak. Handl. Band. 24, 1–39.

Lijklema, L., 1980. Interaction of ortho-phosphate with iron(iii) and aluminum hydroxides. Environ. Sci. Technol. 14, 537–541. http://dx.doi.org/10.1021/es60165a013.

Luedecke, C., Hermanowicz, S., Jenkins, D., 1989. Precipitation of ferric phosphate in activated-sludge – a chemical-model and its verification. Water Sci. Technol. 21, 325–337.

Loewenthal, R., Ekama, G.A., Marais Gv, R., 1989. Mixed weak acid-base systems. 1. Mixture characterization. Water SA 15, 3–24.

McNaught, A.D., Wilkinson, A., 1997. IUPAC Compendium of Chemical Technology. Blackwell Science, Oxford, United Kingdom.

Musvoto, E., Wentzel, M., Loewenthal, R., Ekama, G., 2000. Integrated chemical-physical processes modelling – I. Development of a kinetic-based model for mixed weak acid/base systems. Water Res. 34, 1857–1867. http://dx.doi.org/10.1016/S0043-1354(99)00334-6.

National Institute of Standards and Technology, 2001. NIST Standard Reference Database, vol. 46. Gaithersburg, MD, U.S.A.

Parkhurst, D.L., Thorstenson, D.C., Plummer, L.N., 1980. PHREEQC – a Computer Program for Geochemical Calculations. In: US Geol Surv Water Resour Invest Rep, vol. 80, pp. 210–219.

Pham, A.N., Rose, A.L., Feitz, A.J., Waite, T.D., 2006. Kinetics of Fe(III) precipitation in aqueous solutions at pH 6.0–9.5 and 25°C. Geochim. Cosmochim. Acta 70, 640–650. http://dx.doi.org/10.1016/j.gca.2005.10.018.

Qiu, H., Lv, L., Pan, B., Zhang, Q., Zhang, W., Zhang, Q., 2009. Critical review in adsorption kinetic models. J. Zhejiang Univ.-Sci. A 10, 716–724. http://dx.doi.org/10.1631/jzus.A0820524.

Rahnemaie, R., Hiemstra, T., van Riemsdijk, W.H., 2007. Carbonate adsorption on goethite in competition with

phosphate. J. Colloid Interface Sci. 315, 415–425. http://dx.doi.org/10.1016/j.jcis.2007.07.017.

Reichert, P., 1994. Aquasim – a tool for simulation and data analysis of aquatic systems. Water Sci. Technol. 30, 21–30.

Rose, A.L., Waite, T.D., 2003. Kinetics of hydrolysis and precipitation of ferric iron in seawater. Environ. Sci. Technol. 37, 3897–3903. http://dx.doi.org/10.1021/es034102b.

Smith, S., Takács, I., Murthy, S., Daigger, G.T., Szabo, A., 2008. Phosphate complexation model and its implications for chemical phosphorus removal. Water Environ. Res. 80, 428–438.

Szabo, A., Takács, I., Murthy, S., Daigger, G.T., Licsko, I., Smith, S., 2008. Significance of design and operational variables in chemical phosphorus removal. Water Environ. Res. 80, 407–416. http://dx.doi.org/10.2175/106143008X268498.

Thomas, D.N., Judd, S.J., Fawcett, N., 1999. Flocculation modelling: a review. Water Res. 33, 1579–1592. http://dx.doi.org/10.1016/S0043-1354(98)00392-3.

Vanni, M., 2000. Approximate population balance equations for aggregation–breakage processes. J. Colloid Interface Sci. 221, 143–160. http://dx.doi.org/10.1006/jcis.1999.6571.